Emulsion Studies of Cosmic-Ray Stars Produced in Metal Foils*

IAN G. BARBOUR
Kalamazoo College, Kalamazoo, Michigan
(Received September 1, 1953)

A method is described in which cosmic-ray induced disintegration of nuclei of several elements are studied with metal foils sandwiched between nuclear emulsions placed face-to-face and exposed at balloon altitudes. The range distributions of low-energy particles are obtained from tracks ending in the emulsion. Calculation of the probabilities of detecting star particles permits conversion of the observed star size distributions to the real size distributions, whose variation with atomic number is presented. The variation, with atomic weight, of the cross-sections for the production of stars of various sizes is analyzed. The number of tracks per star corresponding to protons in the energy range 25–100 Mev is obtained and found to vary approximately as the nuclear radius.

I. INTRODUCTION

THE interaction of a high-energy particle with a nucleus appears to be characterized by three major processes: (1) high-energy inelastic processes in which new particles are created (e.g., π-meson production in the collision of an incident nucleon with one or more nucleons in the target nucleus); (2) a "knock-on" process or "nuclear cascade" in which particles of moderate energy are ejected; (3) a final process in which any particles, associated with these interactions, whose energies have degraded until they cannot escape from the nucleus, contribute to the excitation of the whole nucleus and its "evaporation" of low-energy particles. Insight into the operation of all three types of interaction may be expected from investigation of how various characteristics of nuclear disintegrations depend on the atomic number of the target nucleus. Because photographic emulsions include a variety of elements, it is often impossible to ascribe with certainty to the disintegration of the nucleus of a particular element an individual event observed in an ordinary emulsion;[1] knowledge of how star characteristics vary with the atomic number of the nucleus is thus also of importance in interpreting existing data on stars in emulsions, as well as in understanding the nuclear interaction processes themselves. This paper will: (a) describe an experiment designed to study disintegrations in various elements; (b) present data on size distributions and cross-sections; and (c) analyze the data on particles ejected at moderate energies and their relation to the second or "knock-on" process mentioned above. Data relevant to the other two types of interaction will be presented at a later date.

* This work has been aided by a Cottrell Grant from the Research Corporation.

[1] The principal exceptions are: (a) there exist stars of more than seven heavy prongs which can be attributed to Ag or Br; (b) there exist stars of less than six heavy prongs *plus* a minimum-ionization shower, which have been attributed by some authors to the group of lighter elements [see L. S. Osborne, Phys. Rev. **81**, 238 (1951)]; (c) an attempt has been made to differentiate certain stars from the capture of negative π mesons on the basis of the presence of Auger electrons or of α particles of energy less than the potential barrier for bromine [see Menon, Muirhead, and Rochat, Phil. Mag. **41**, 583 (1950)]; (d) Harding [Phil. Mag. **40**, 530 (1949)] has shown that stars with recoil fragments are mostly due the disintegration of Ag or Br.

The comparison of stars in ordinary emulsions with those occurring in emulsions "loaded" with transparent salts does not allow an unambiguous interpretation of each observed event and requires exceptionally good statistics if the differences are to be reliable. Harding[2] attempted to avoid this difficulty by studying stars produced in alternated layers of pure gelatin and standard emulsion; this method is valuable but can be used to study stars produced only in a certain group of light elements. In our initial attempt to introduce small but visible particles of metal within the emulsion, we found that quantities in excess of about 2 percent by volume interfere with the scanning of the plates. In the method finally adopted after having overcome a number of practical difficulties, thin foils of various metals were "sandwiched" between pairs of plates placed face-to-face; the procedure has been briefly described and preliminary results communicated.[3] More recently Hodgson[4] has reported analysis of stars from the disintegration of nuclei of a lead plate in contact with a single photographic emulsion. Some results of an experiment using the "sandwich" method have also been reported by Setti and Merlin.[5]

II. EXPERIMENTAL PROCEDURE

1. Preparation and Exposure

Six metal foils with thicknesses as follows were used in this investigation: Au (51μ); Pt (25μ); Sn (36μ); Cu (43μ); Ni (23μ); and Al (51μ). Ilford G5 200μ emulsions, 2 in.$\times$4 in., were employed. Although more accurate energy measurements at low energies and better discrimination between alpha particles and protons could have been obtained with less sensitive emulsions, such as C2, it seemed desirable to use "minimum ionization" plates in order to record the star particles of higher energy. It was found in preliminary experiments that, even under the maximum pressure which could be applied safely without breaking the glass backing of the plates, the foils would not lie flat

[2] J. B. Harding, Nature **163**, 440 (1949).
[3] I. Barbour and L. Greene, Phys. Rev. **79**, 406 (1950); I. Barbour, Phys. Rev. **82**, 280 (1951).
[4] P. E. Hodgson, Phil. Mag. **42**, 92 (1951).
[5] R. Setti and M. Merlin, Nuovo cimento **8**, 504 (1951).

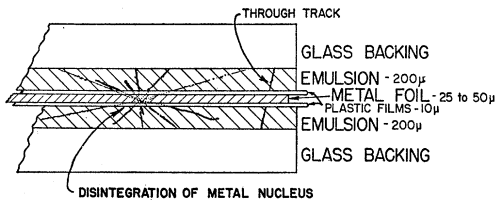

FIG. 1. Cross-sectional diagram of emulsion "sandwich" showing how tracks from the disintegration of a metal nucleus are recorded in the emulsion on either side of the foil. A "through" track is also depicted for comparison.

enough to insure good contact; for if the two emulsion surfaces are more than about 100μ apart during exposure, the particles from disintegrations in the foil may have diverged so much before striking the emulsion that a substantial fraction will be located in the emulsion outside the microscope field-of-view and will be missed during scanning of the plates. It was found desirable therefore to give each foil a preliminary treatment by heating to its annealing temperature in a furnace to render it malleable and then subjecting it to a pressure of $\sim$1 ton/in.^{2} between two very flat steel surfaces. The foils thus flattened were placed between 10μ sheets of cellophane to prevent interaction of the metal atoms with those of the emulsion, and included between pairs of photographic plates as indicated in Fig. 1.

Each such "sandwich" was then placed between two $\frac{3}{16}$-inch aluminum plates which, when fitted into a yoke containing setscrews, could be clamped together to insure good contact and prevent the plates from slipping during exposure. The corners of one of the aluminum plates as well as those of the foil had been cut off to allow a system of registration dots to be imprinted on each pair of emulsions in order to facilitate realignment after development; these registration marks were imprinted[6] by interposing a $\frac{1}{32}$-inch Pb plate drilled with 100μ holes between the sandwich and a distant x-ray source.

A small gondola containing these plate assemblies was attached to a "Skyhook" balloon load-line 40 feet from any other apparatus, and was flown[7] at 55° N geomagnetic latitude for six hours at 93 000 feet. After removal of the foils, the plates were developed by the familiar "two-temperature" method. Each pair of "matching" plates was then in turn placed emulsion-to-emulsion on the microscope stage for re-alignment.

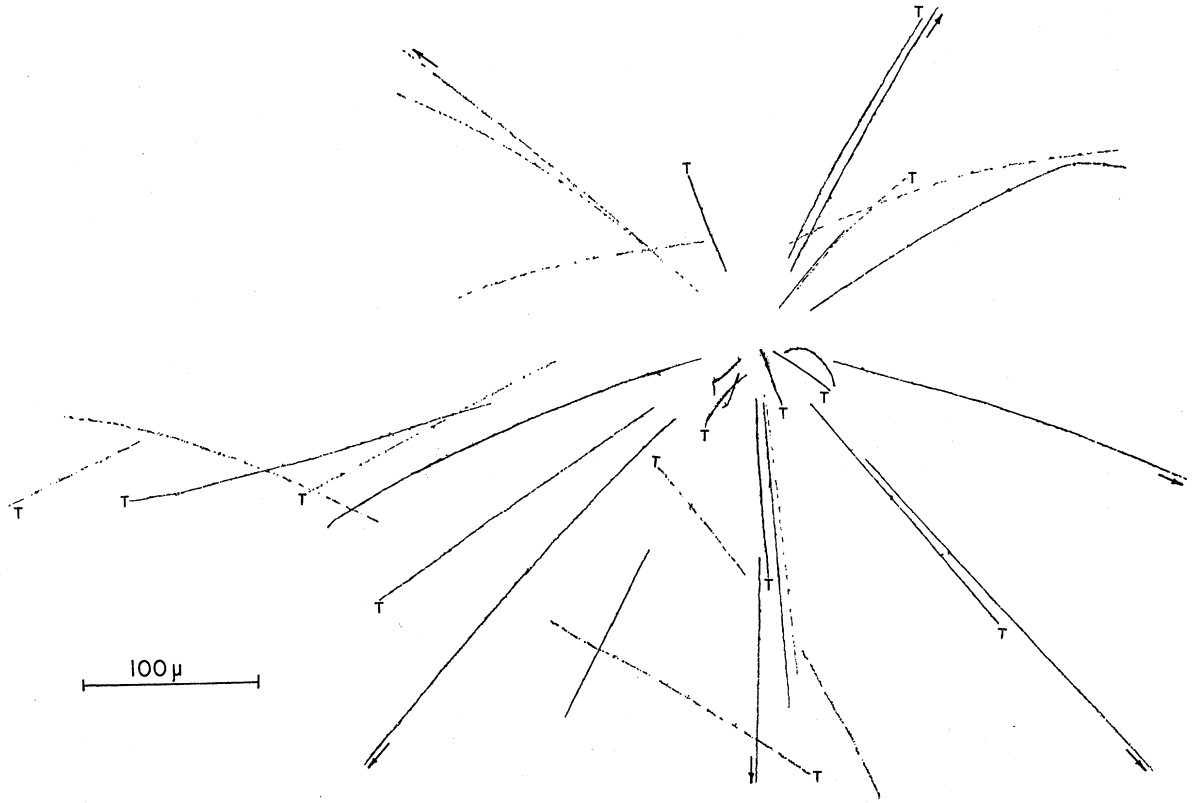

FIG. 2. Microprojection tracing of 24 tracks from the disintegration of a gold nucleus. Tracks marked "*T*" were found in the top plate, others in the bottom plate. Arrows indicate tracks continuing in the emulsion beyond the limits of the tracing. Several matching "through" tracks not associated with the star are also present.

[6] I. Barbour, Phys. Rev. **78**, 518 (1950).
[7] Arranged through the kindness of the U. S. Office of Naval Research and General Mills, Inc.

The x-ray dots allowed approximate reconstruction of the original relative orientation of the two plates; exact realignment was achieved by painstakingly touching the top plate at appropriate points with a micrometer-screw adjustment until the "matching" segments of high-energy "through" tracks in all portions of the plates were aligned to within a few microns (except where distorted at the plate edges). Weights were then placed on the top plate to hold the two emulsions in close contact and in this position each pair of plates was cemented together for scanning.

2. Scanning

The two juxtaposed emulsion layers of each pair of plates were scanned at a magnification of 200×. A typical foil star and "through" tracks are shown in Fig. 2. Scanning for tracks from the disintegration of foil nuclei is accomplished in two ways simultaneously: (a) positively, the scanner looks in the double emulsion for groups of three or more tracks which appear to diverge from a common center between the emulsion surfaces, and (b) negatively, he can, for each and every track observed in the emulsion, look for a continuation in the "matching" plate which would eliminate that track from consideration as a possible member of a foil star. (An occasional cosmic-ray particle stopping in the foil will, of course, leave a track in one emulsion only, but the scanner will at least have been alerted to look for a possible foil star.) The use of two emulsions thus appears to have several advantages over foil experiments using only one plate: (1) there is twice the probability of detecting a particle from a foil star; (2) fewer foil stars will be missed since every single track observed can be examined and the majority rejected as "through" tracks by method (b) above; (3) cases of the random crossing of 2 or 3 "through" tracks, which on one plate might erroneously be interpreted as due to a foil star, can be eliminated; (4) the probability of missing a particle from an observed foil star is, as shown below, almost independent of the point within the foil at which the star occurs, since the increased detection-probability for tracks in the plate nearer the disintegrating nucleus is compensated for by the decreased detection-probability in the further plate.

After the plates had been scanned, each event of interest was examined under 450× magnification (using a 30× objective of large working distance to observe through the glass backing of the top plate), and an approximate scale drawing was made of each foil star and all the tracks in its neighborhood, by use of an eyepiece protractor. Finally each pair of plates was separated and both halves of every foil star were examined under oil, to search for tracks which might have been missed at lower magnification and to obtain for each track data such as grain density, horizontal and vertical projection of track length, and distance from the point of entering the emulsion to the star "center."

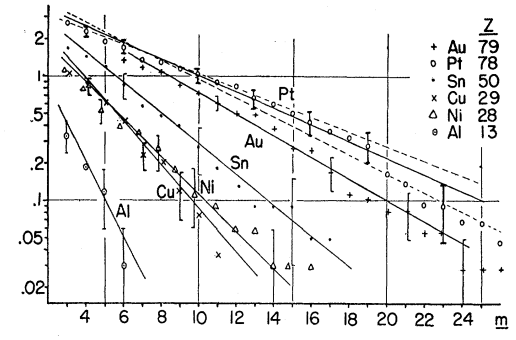

FIG. 3. Observed star-size distributions: relative number of stars observed, per target nucleus, with m or more observed prongs (excluding min ionization tracks) per star, plotted against m for various foils.

III. FOIL STAR DATA AND DETECTION PROBABILITIES

1. Observed Size Distributions

The uncorrected integral star-size distributions observed are shown in Fig. 3, where for each foil the number of stars observed with m or more observed prongs per target nucleus is plotted logarithmically against m. Throughout this analysis, "minimum ionization" tracks of grain density <1.5 times minimum have not been included in describing star size. Typical statistical probable errors are indicated in the graph, as well as limits for the best straight-line fit from which were found constants of a distribution of the form $M(m)=M_0e^{-\lambda m}$. (The low experimental values for stars of $m\leqslant 5$ can be attributed to inefficiency in detecting small stars; although this error due to missing small stars has been estimated by having a second observer rescan sample areas with very great care, the data must be considered less reliable with respect to small stars than large ones. This error of completely missing stars should not be confused with failure to detect additional particles produced in observed stars, an effect for which correction can be made rather rigorously, as discussed in the ensuing paragraphs.)

2. Observed and Real Range Distributions

For each particle observed to stop in the emulsion, an equivalent total range R in emulsion was calculated from the relative stopping power of foil, cellophane, and emulsion, using the various angle and distance data on each track. The real production spectrum was obtained from the observed number of prongs of equivalent range R by dividing by $S(R)$, the probability that a prong of equivalent range R will be detected as a track stopping in the emulsion, calculated for each foil as follows. Consider for the moment one emulsion, and assume that these stopping particles are emitted isotropically. Let f be the distance of the star center from the emulsion surface, θ the original dip angle of a track measured from the line through the star center perpendicular to the emulsion surface, and $r=f\tan\theta$ the distance along

the emulsion surface from the foot of that perpendicular to the point where the particle enters the emulsion. Now a particle with a given equivalent range R will in general pass through the emulsion only if its angle θ is less than some minimum value $\theta_{\min}(R,f,Z)$; on the other hand, it will stop in the foil or cellophane and never enter the emulsion if θ exceeds a value $\theta_{\max}(R,f,Z)$. Only particles for which $\theta_{\min}<\theta<\theta_{\max}$ will stop in the emulsion. (These limiting angles are readily calculable for each foil from geometrical considerations, if the relative stopping powers[8] involved are given and the original emulsion thickness is assumed to be 200μ.) The probability of detecting a particle of equivalent range R as a track stopping in the emulsion is then given by

$$S_f(R)=\int_{\theta_{\min}}^{\theta_{\max}} D(f\tan\theta)\cdot\tfrac{1}{2}\sin\theta d\theta, \qquad (1)$$

where $D(f\tan\theta)$ is the scanning efficiency or probability of actually observing a track which enters the emulsion at a distance $r=f\tan\theta$ from the foot of the perpendicular through the star center.

The scanning efficiency $D(r)$ depends on the magnification and care used in examining the region in which the star is located. To obtain an analytic expression for the above integral, we have assumed $D(r)=1$ for $r<100\mu$, thereafter dropping uniformly to zero at $r=250\mu$, which is about the greatest distance at which a particle is likely to be detected at our magnification.[9] Such an assumption for $D(r)$ is consistent with the experimental data. Figure 4, for instance, shows for a sampling from Pt, the curve of the theoretical distribution-in-r (the number of tracks which would be expected to enter the emulsion at a distance r from the perpendicular through the star center, calculated on the basis of isotropy and averaged over the various f values or depths in the foil, with allowance for particles stopped in the foil as found below); experimental points are plotted for the number of tracks actually observed in various intervals of r. The decrease in experimental values as compared with the theoretical curve for $r>100\mu$ is consistent with the assumed scanning efficiency function, $D(r)$.

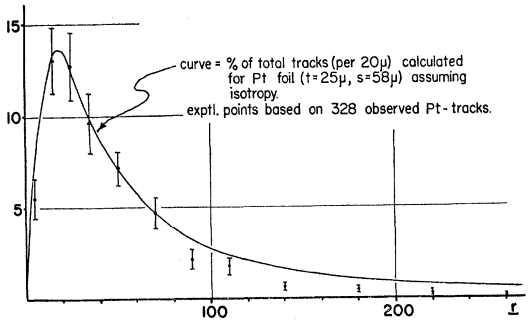

FIG. 4. Number of tracks from Pt-stars observed to enter emulsion at a distance r from the star "center," per 20μ interval of r. (r is measured along the emulsion surface from the point at which a track enters the emulsion to the line perpendicular to the emulsion surface through the star center.) The theoretical curve (assuming 100 percent scanning efficiency) allows for tracks stopping in the foil (see text).

The average probability $S(R)$ of detecting a particle of equivalent range R as a track stopping in the emulsion can thus be obtained for each foil by evaluating the expression in Eq. (1) and then integrating numerically over f, the various depths in the foil at which the star could occur, for both plates. Taking the observed number of prongs of equivalent range R and dividing by the probability function $S(R)$, one can now obtain the real range distribution $\nu(R)$, as given in Fig. 5 for several foils. Stopped particles from a sampling of emulsion stars of 8 or more prongs are the basis for the spectrum of "Ag+Br" (weighted again by an appropriate probability function which for tracks both beginning and ending in the emulsion is readily calculated from geometric considerations). The preponderance of short prongs in the lighter elements is attributable to their lower barrier.

3. Total Detection Probabilities

The total probability $P(R)$ of detecting a particle of equivalent range R (i.e., observing it as a particle stopping in the emulsion or passing through it) is calculated in an analgous way for each foil, with the lower limit in Eq. (1) replaced by zero since here particles passing through the emulsion are to be included. The resulting total probability for two plates is almost independent of f, the distance of the star center from one emulsion surface. [Because the increased probability of detection in the plate nearer the star center is almost exactly compensated for by the decreased probability in the opposite emulsion, the same $P(R)$ values can be used for all stars in a given foil, simplifying the calculations greatly.] Now for each foil $P(R)$ is found to be constant (to within 2 percent) above $R\cong 250\mu$ [essentially because the integral in Eq. (1) is insensitive to $\theta_{\max}(R,f)$ once the scanning efficiency $D(f\tan\theta)$ has dropped to zero; in other words, particles of long range are lost by stoppage in the foil only at angles where they would in any case have escaped detection beyond the limits of the field-of-view]. This limiting value of $P(R)$, which we may call P_∞, the probability of detecting an energetic particle, is determined largely by the average solid angle which the fields-of-view of the two emulsion surfaces subtend from the star center and to a lesser extent by the loss of scanning efficiency $D(r)$

[8] H. Yagoda, *Radioactive Measurements with Nuclear Emulsions* (John Wiley and Sons, Inc., New York, 1949).

[9] Although the radius of the field of view in scanning was 250μ, a *greater* region around each star was examined by placing the star center successively at various points on the periphery of the field-of-view. On the other hand, the region which can be examined effectively under oil is considerably *smaller*. There is also evidence (see Fig. 4) that some steep tracks, mostly of low grain density, are missed. The assumed scanning efficiency function $D(r)$ represents a reasonable compromise of these factors.

near the edges of the field of view; P_∞ has values of 0.7 to 0.8 for the various foil thicknesses used. At the other extreme, $P(R)$ of course approaches zero as $R\rightarrow 0$, due to losses in the foil.

The total detection probability P for all particles is

$$P=\int_0^\infty P(R)\nu(R)dR \Big/ \int_0^\infty \nu(R)dR, \qquad (2)$$

where, as before, $\nu(R)$ is the real range distribution. This can most conveniently be expressed in the form $P=P_\infty/(1+C/L)$, where L is the total number of observed tracks and C, the number of additional particles missed because of stoppage in the foil at angles where they might otherwise have been detected, is given by

$$C=\int_0^{250} \nu(R)[P_\infty-P(R)]dR. \qquad (3)$$

Only the portion of the range distribution below 250μ is needed here, as above that value $P(R)\cong P_\infty$; the correction C/L amounts to 3 to 5 percent in the various foils. [Actually the α/p ratio[10] and the fraction of particles observed to stop in the emulsion do vary somewhat with star size, so that a separate range distribution $\nu(R)$ and correction C should be worked out for groups of stars of different sizes in each foil; we are justified, however, in using an average value of P for stars of all sizes since C is in any case a small correction to P_∞.]

IV. CONVERSION FROM OBSERVED TO REAL SIZE DISTRIBUTIONS

Having obtained for each foil the over-all detection probability P, the observed size distribution $M(m)$ can be used to calculate the real size distribution, $N(n)$ (the original distribution as produced at the nucleus), where m and n are the number of observed and real prongs respectively. Assume that the real integral distribution of stars of n or more prongs is given by $N=N_0e^{-\xi n}$, giving a real differential distribution $N'(n)=\xi N_0e^{-\xi n}$ stars of n prongs. If the probability of observing an individual track is P, then the probability[11] that an n prong star will be observed as an m prong star is given by

$$p(n,m)=\frac{n!}{m!(n-m)!}P^m(1-P)^{n-m}. \qquad (4)$$

Now the total number of m-prong stars to be expected will be $M'(m)=\sum_n p(n,m)N'(n)$. Substituting the values of $p(n,m)$ and $N'(n)$ above, the resulting sum may be evaluated analytically if summed over values of n from m to infinity [a procedure which is justified, despite the obvious upper limit to n set by the size of the nucleus disintegrating, because $p(n,m)$ is small for $n\gg m$, and also $N'(n)$ drops to a negligible value as n approaches its actual upper limit]. When the sum is evaluated, the resulting observed differential distribution $M'(m)$ is found to be exponential, giving an expression for the observed integral distribution to be expected of the form $M(m)=M_0e^{-\lambda m}$, where the constants are functions of the original parameters ξ, N_0, and P. In practice, however, instead of calculating the *observed* distribution to be expected from a given *real* distribution, one's objective is just the reverse. The constants of the real integral distribution, in terms of those observed, are found to be: $\xi=\ln[Pe^\lambda+(1-P)]$ and $N_0=(M_0\lambda/\xi)\times[1-(1-P)e^{-\xi}]$. For $P>0.7$, the former expression differs only slightly from the value $\xi=\lambda P$ which would hold if all n prong stars were to be observed as stars of exactly nP prongs, rather that the correct probability spread around this value given by Eq. (4) above.

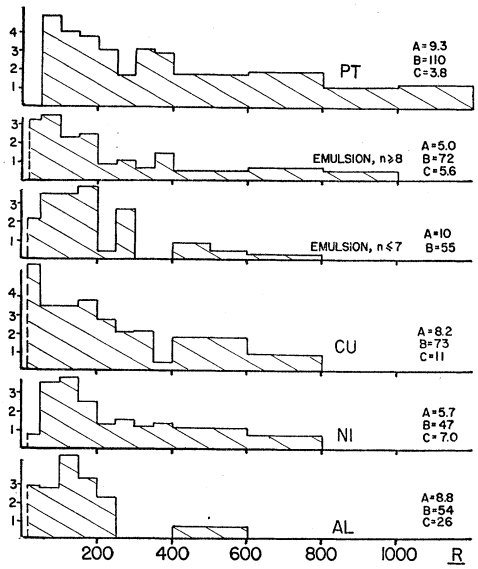

FIG. 5. Range distributions $\nu(R)$ of particles observed to stop in the emulsion for various foils. Number of particles of equivalent emulsion range R, per interval of 50μ in R, corrected as indicated in the text for detection probability and for the portion of the trajectory of each particle in the foil. (To compare the number of particles *per star*, divide the ordinates by the factor A; to compare number of particles *per target nucleus*, divide by $B(\times 10^{20})$; to compare number of particles *per real star track*, divide by C.)

V. REAL SIZE DISTRIBUTIONS

The value of the exponent ξ of the real size distribution, calculated for each foil from the exponent λ of the observed distribution (Fig. 3) and the detection probability P (Sec. III–3 above) by the conversion formulas just developed (Sec. IV), is plotted[12] as a function of the

[10] See also D. Perkins, Phil. Mag. **41**, 138 (1950).

[11] See also reference 4 above.

[12] Probable errors shown represent the extreme slopes of distributions drawn at the limits of statistical probable errors of individual points, as illustrated for Pt in Fig. 3. With respect to both foil star data and the emulsion star analysis discussed below, the values for *lighter* elements are more uncertain than those for heavier elements because estimation of the scanning inefficiency for 3-, 4-, or 5-prong stars results in a greater uncertainty for small nuclei. Failure to detect very small stars originating in either the foil or the emulsion would result in an under estimation of the value of ξ for elements of low atomic number.

atomic number in Fig. 6. We have also plotted points corresponding to the two groups of emulsion constituents, calculated in the following manner. The distribution for stars observed with centers in the emulsion is shown in Fig. 7, and exhibits the characteristic break at about $n=7$. Now this change of slope in the distributions of emulsion stars has previously been interpreted in three ways. Barton *et al.*[13] consider this effect as fortuitous. Bernadini *et al.*[14] attribute the change of slope to the presence of the low-energy component in the incident cosmic-radiation. Page,[15] and Birnbaum *et al.*[16] attribute the effect to the presence of elements of low atomic number in the emulsion. The latter interpretation is favored by the essential linearity of our logarithmic plots for a *single* element, such as the Pt-foil data of Fig. 3; however, because of the low scanning efficiency for small stars, a small nonlinearity in the distribution from a single element cannot be ruled out. The results of the following analysis of the emulsion stars, which assumes the latter interpretation, are consistent with the foil star data [see Fig. 8]. The emulsion contains a group of heavy elements (Ag and Br) of average atomic weight 94, and a light group (chiefly C, N, O) of average atomic weight 14. If then ξ_1 and ξ_2 are the slopes of the two portions of the curve in Fig. 7, and we assume that portion 2 and its extrapolation is contributed by the group of heavy elements, then the slope of the star distribution contributed by the group of light elements is calculated to be $\xi_L \cong K(\xi_1-\xi_2)(K-1)$, where $K=e^{7(\xi_1-\xi_2)}$. The values obtained in this way for the heavy and light emulsion groups, on the basis of our data, as well as those calculated by this same method from the emulsion star

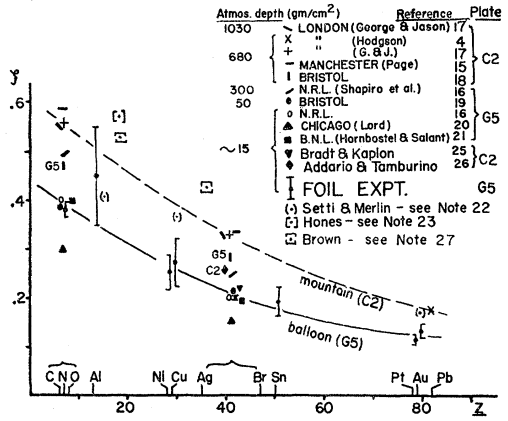

FIG. 6. Exponent, ξ, of real star size distributions, plotted as a function of atomic number. Values obtained from the data of other observers by the method described in the text are shown for comparison. (References given as indicated, in footnotes.)

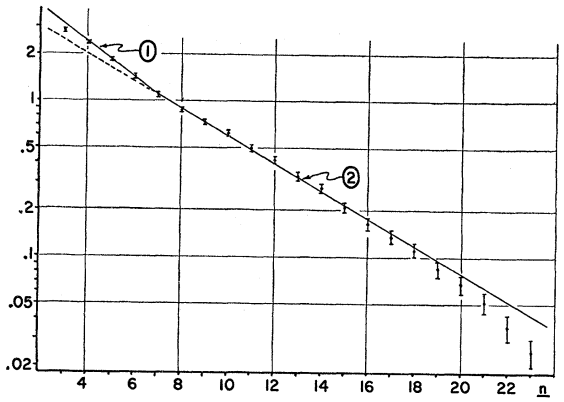

FIG. 7. Relative integral star-size distribution for stars with centers in the emulsion (number of emulsion stars of n or more prongs).

data given by a number of other observers,[15–27] are plotted in Fig. 6.

Hodgson's value[4] obtained with a Pb plate is also given in this graph. We have calculated very rough values shown in brackets from the data of Setti and Merlin.[22] Harding's gelatin-layer data[2] yield $\xi \sim 0.9$ for the C—N—O group; this value is higher than the other data, but is based on a small number of stars. Data obtained on cloud-chamber stars by Hones[23] using argon at sea level and by Brown[27] at mountain altitudes are the basis of other values plotted in Fig. 6. In general, the effect of the difference in the incident energy spectrum at balloon and mountain altitudes is clearly reflected in the graph.[24] Results at cyclotron energies give even higher values for the slope of the star-size distributions. Bernadini's data[28] yields a value ~ 0.8 for emulsion stars produced by 385-Mev protons; cloud chamber measurements by Bøggild and Tenney[29] with

[13] Barton, George, and Jason, Proc. Phys. Soc. (London) **A64**, 175 (1951).
[14] Bernadini, Cortini, and Manfredini, Phys. Rev. **79**, 952 (1950).
[15] N. Page, Proc. Phys. Soc. (London) **A63**, 250 (1950).
[16] Birnbaum, Shapiro, Stiller, and O'Dell, Phys. Rev. **86**, 86 (1952).
[17] E. George and A. Jason, Proc. Phys. Soc. **A62**, 243 (1949).
[18] Brown, Camerini, Fowler, Heitler, King, and Powell, Phil. Mag. **40**, 862 (1949).
[19] Camerini, Davies, Fowler, Franzinetti, Muirhead, Lock, Perkins, and Hekutieli, Phil. Mag. **42**, 1241 (1951).
[20] J. Lord, Phys. Rev. **81**, 901 (1951).
[21] J. Hornbostel and E. O. Salant, quoted in reference 16.
[22] Reference 5. G5 emulsions at 4450 m. Their method of converting from observed to real distribution does not appear to us valid; we have instead used their observed data together with very rough estimates of their detection probabilities to obtain by the method of Sec. IV the three very approximate values plotted in brackets.
[23] E. Hones, Phys. Rev. **83**, 1263 (1951) and private communication. Cloud chamber stars in argon at sea level; triggering was with built-in ionization chamber.
[24] The points on the graph representing C2 data are invariably somewhat higher than those from G5 data under the same conditions. This may be attributed to the insensitivity of C2 emulsions to the high energy particles occurring more frequently in large stars (see references 18 and 19), resulting in a steeper size-frequency distribution in C2.
[25] H. Bradt and M. Kaplon, Phys. Rev. **78**, 680 (1950).
[26] M. Addario and S. Tamburino, Phys. Rev. **76**, 983 (1949).
[27] F. Brown (private communication and Princeton University thesis). Cloud ion-chamber data at mountain altitude (700 g/cm²). Probable errors quoted are ~10 percent; singly charged particles of ~2.5 minimum ionization were recorded.
[28] Bernadini, Booth, and Lindebaum, Phys. Rev. **80**, 905 (1950).
[29] J. Bøggild and F. Tenney, Phys. Rev. **84**, 1070 (1951).

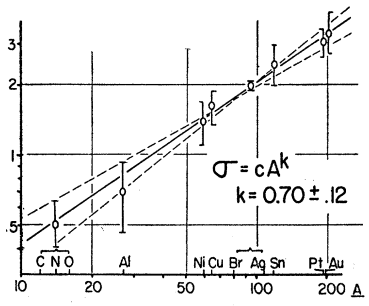

FIG. 8. Number of stars (per target nucleus) with 4 of more real prongs, plotted against the atomic weight of the target. The derivation of the points representing the emulsion constitutents is explained in the text.

190-Mev neutrons give values around 0.9 for krypton and oxygen, whereas for 90-Mev neutrons in alcohol and water vapor, Horning's data[30] would give a value of about 1.2.

VI. STAR-PRODUCTION CROSS SECTIONS

From the values of N_0 and ξ, calculated for the real star size distributions of each element, the star-production cross sections may be computed. The relative integral cross sections for all stars of four or more real prongs are shown in Fig. 8. (Probable errors include uncertainty in ξ, as well as statistical errors in number of stars observed.) Values for stars in the emulsion were obtained as follows. The ratio of the observed number of emulsion stars of $n \geqslant 3$ to the number of stars of three or more prongs attributable to Ag and Br is found by extrapolation of curve 2, Fig. 7. Averaging our value of this ratio with that obtainable from the star populations of other observers (see values quoted in reference 16) gives an average of $\sim 1.43 \pm 0.1$ for this ratio. Using the chemical analysis of the emulsion as supplied by the manufacturer, the cross sections for stars of $n \geqslant 4$ in the light and heavy emulsion groups can be calculated, and is plotted also in Fig. 8. If the observed exponential size distributions (*e.g.*, straight-line curves in Fig. 3) are assumed to hold down to the smallest stars, the cross sections for stars of $n \geqslant 1$ as a function of atomic weight would fall on a line of somewhat less steep slope ($\sim A^{\frac{1}{3}}$). This would involve a rather great extrapolation beyond the smallest stars observable in our foil experiments ($m=3$ or $n=4$). Even for emulsion stars, scanning efficiency for $n \leqslant 3$ is low, and most observers do not quote results for $n=1$ or 2 because of the ambiguity in interpreting such events.[31]

Although comparison with experiments of other observers where different energy spectra are involved may be of little value, it might be noted that Brown[27] finds for cloud ion chamber stars size distributions varying uniformly down to the smallest stars, and also finds for stars of $n \geqslant 2$ a variation with atomic weight less rapid than $A^{\frac{2}{3}}$. These cross sections should not in any case be interpreted as total interaction cross sections, which would have to include "stars" of zero-prongs and other processes whereby the star-producing radiation is absorbed.[32] Other experimeters[33] have reported results consistent with a geometric cross section for the total absorption of the star-production radiation under lead, air, ice, etc. Experiments on the production of bursts in ionization chambers of various wall materials[34] and the study of stars produced in emulsions with gelatin layers[2] have also shown an approximately geometrical variation. Blau and Oliver[35] have more recently exposed gelatin layers to 300-Mev neutrons and find evidence for some nuclear transparency.

VII. THE GRAY-BLACK TRACKS

1. Experimental Results

In the preceding sections we have been considering all particles except shower particles (<1.5 min). We turn now to the analysis of a particular group of particles, the "gray-black" tracks of density from 3 to 7 times minimum ionization, corresponding to protons of energy from 25 to 100 Mev. Every foil star track (except those making an angle of more than 60° with the emulsion surface) was grain-counted, and those with corrected grain counts falling near the boundaries of the above interval were rechecked. Calibration was established by grain counts on very long mesons coming to rest in the emulsion. The average number of gray-black tracks per star (corrected for detection efficiency) is shown for various elements and star sizes in Table I. Here, as throughout, star size refers to the number of prongs with >1.5 min ionization. The data for Ag+Br

TABLE I. Values for the average number of gray-black tracks per star, classified according to star size (vertical columns) and target material (horizontal lines).

m (obs. prongs) / n (real prongs)	3–4	3–5 / 5–7	6–9 / 8–13	10–13 / 14–19	14–20 / 20–30	All stars
Emulsion	1.2 ± 0.3	1.2 ± 0.2	3.1 ± 0.6	3.8 ± 0.7	6.8 ± 0.8	2.0 ± 0.2
Pt		1.2 ± 0.2	$3.4 + 0.6$	4.9 ± 0.8	6.2 ± 0.7	2.9 ± 0.2
Ag and Br			3.1 ± 0.6	3.8 ± 0.7	6.8 ± 0.8	(2.1 ± 0.3)
Cu		1.9 ± 0.4	2.5 ± 0.5	6.4 ± 1.6		1.9 ± 0.3
Ni		1.7 ± 0.4	3.0 ± 0.7	5.7 ± 1.7	7.1 ± 3.2	2.0 ± 0.3
Al		1.2 ± 0.5	3.5 ± 2.5			1.4 ± 0.4
C, N, O	(1.2)	(1.3)				(1.2)
Average	(1.2)	1.3	2.9	4.6	6.4	

[30] W. Horning, Phys. Rev. **75**, 378 (1949).

[31] C. Lees *et al.* [Lees, Morrison, Muirhead, Rosser, Phil. Mag. 44, 304 (1953)] have recently reported comparison of "diluted" and normal emulsions, bombarded with 120-Mev protons. Using "along the track" scanning, they find many more stars of 0, 1, and 2 outgoing particles attribtable to heavy than to light elements at these low energies.

[32] There is also low-energy secondary radiation present which will be effective in producing stars in the light elements but not in the heavier elements with higher Coulomb barriers. A low-energy neutron may produce a star of 3 or 4 particles in a light nucleus because of the low binding energy for alpha particles.

[33] D. George, Nature **162**, 333 (1948); J. Harding and J. Lattimore, Nature **163**, 319 (1949); and reference 17 above.

[34] H. Lewis, Phys. Rev. **78**, 483 (1950).

[35] M. Blau and A. Oliver, Phys. Rev. **87**, 182 (1952).

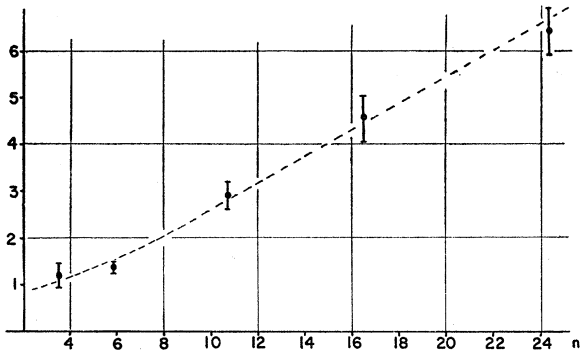

FIG. 9. Number of gray-black tracks per star, averaged over all stars of a given size in all the foils, as a function of star size. n is the number of real tracks with ionization >1.5 min.

were obtained from large stars in the emulsion (top line).[36]

It can be seen that the number of gray-black tracks per star increases with star size, indicating the increase in excitation energy accompanying the process which gives rise to more knock-ons, as discussed below. There is little variation with Z in the number of gray-black tracks per star *for stars of a given size* (vertical columns); the variation in the values averaged for all stars in a given element (last column) arises primarily from the varying distributions of the star population among the star size groups for various elements. The number of gray-black tracks per star of a given size (average for all elements weighted as inverse square of prob. errors, as shown in the bottom line of Table I) is plotted against star size in Fig. 9. Comparable values by Brown *et al.*[18] for "grey" tracks are uniformly ~25 percent lower; however, their "grey" tracks refer to a slightly different energy interval (1.5 to 5 times min) and were obtained at mountain altitudes. The mountain data of Bernadini *et al.*[14] for protons in the interval 80–300 Mev would give a curve about 50 percent lower. At cyclotron energies (400 Mev), Bernadini, Booth, and Lindebaum[37] report an average of 0.35 tracks (per star) in their "sparse-black" group (3 to 6 times minimum, corresponding to 30–100 Mev protons) and a mean of 3.3 prongs per star.[38]

[36] It was found that the ratio of the number of gray-black tracks per star for *all* stars to that for *large* stars only ($m \geqslant 6$ or $\sim n \geqslant 8$) in Pt, Cu, and Ni was almost constant (~1.3). If we assume that this same ratio applies for Ag+Br, the number of gray-black prongs for *all* Ag+Br stars can be estimated as shown in brackets in Table I. The calculation for the light emulsion elements is less reliable; the large Ag+Br star data were first extrapolated to small Ag+Br stars on the basis of the corresponding ratios in the foils, and the fraction of small stars attributable to the light elements obtained from the cross sections (Fig. 8) and emulsion composition. This permitted an estimate to be made of the number of gray-black tracks per star attributable to C, N, and O.

[37] Bernadini, Booth, and Lindebnaum, Phys. Rev. 88, 1017 (1952).

[38] The resulting point would fall about 40 percent below our curve, and their energy interval is nearly the same as ours. However, the situation differs in that the total available energy is constant, so that the more energy escapes in fast protons, the less there is available for evaporation prongs.

The number of *black* tracks (>7 times min) per gray-black track, averaged over the elements, is 3.4, 2.7, 2.6, and 2.8, for stars of 5–7, 8–13, 14–19, and 20–30 real prongs, respectively. It is thus seen that about $2\frac{3}{4}$ black tracks are associated with every gray-black track, and that this number varies little with Z and shows only slight variation with star size.

The average number of gray-black tracks per star averaged over all stars, regardless of size, from a given foil is plotted against the atomic weight in Fig. 10, and is seen to vary approximately as the nuclear radius. While here, as throughout this section, the absolute values are subject to considerable error, the relative values must be considered fairly reliable; since the same scanning and grain-counting techniques were used in all cases, errors due to failure to detect fast particles, or in calibrating grain-counts, tend to effect all foil values approximately equally.

2. Theory and Discussion

Since the gray-black group includes protons only of energies greater than 25 Mev it can contain relatively few evaporation particles. Although the separation is not clear-cut, especially for lighter nuclei (e.g., the Fermi energies ~20 Mev), it is clear that we are dealing primarily with particles ejected at energies higher than those for which evaporation theory can account. Our data also show that the gray-black group has a much greater anisotropy than the tracks of density corresponding to protons of $E<25$ Mev, which also indicates that their origin is not in an evaporation process.

Since we are dealing in the cosmic radiation with particles whose de Broglie wavelength is less than that of the nuclei involved, a semiclassical approach to the theoretical consideration of the origin of these fast protons can be expected to be fairly satisfactory. In this approach, a high-energy nucleon is considered as interacting independently with a single nucleon in the nucleus with the same cross section as a free nucleon-nucleon interaction; each particle from such a collision can in turn collide with other nuclei, or escape from the nucleus. (When any nucleon has insufficient energy to escape, it is considered as contributing to the excitation of the whole nucleus and the subsequent "evaporation.") Goldberger[39] has calculated by the Monte Carlo method

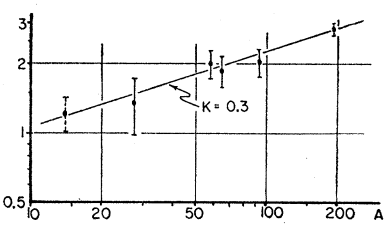

FIG. 10. Average number of gray-black tracks per star (averaged over all stars regardless of size from a given foil) plotted against the atomic weight of the target.

[39] M. Goldberger, Phys. Rev. 74, 1268 (1948).

the effect of the exclusion principle for the nucleon-nucleon collisions resulting when 90-Mev neutrons are incident on such a Fermi gas of nucleons and finds a reduction of the effective cross-section in the ratio of 1 to $(1-7E_F/5E_i)$, where E_F is the Fermi energy and E_i is the energy of the incident neutron. A similar calculation was carried out at 400 Mev by Bernadini *et al.*[37]

According to this model, the mean free path, λ, of a proton in nuclear matter is given by the average proton-nucleon cross sections, namely,[40]

$$1/\lambda = 3F[Z\sigma_{pp} + (A-Z)\sigma_{pn}]/4\pi R^3, \qquad (5)$$

where R is the nuclear radius and F the factor taking into account the effect of the exclusion principle. A similar expression holds for an incident neutron. As a first approximation, λ will not be a function of Z, provided we assume: (a) the density of nuclear matter is constant (as indicated in scattering experiments, such as those of DeJuren and Knable;[41] (b) the effect which the small variation in the A/Z ratio has on the average nucleon-nucleon scattering cross section (averaged over protons and neutrons in the nucleus) can be neglected; and (c) the variation of F with A can be neglected. The last assumption seems justified since the Fermi momentum turns out to be independent of Z, except for a small shift due to the variation in the A/Z ratio; in any case, at these higher energies the exclusion principle, which operates chiefly in forbidding small momentum-transfers, plays a less significant role except in the final stages of any given internal nucleonic cascade. With these assumptions the mean-free-path in the nuclear matter of various elements is a function of energy only.

On this basis one would anticipate that the number of fast protons ejected would increase with nuclear size faster than the nuclear radius, because of cascade action within the nucleus. However, for larger nuclei it is more difficult for a proton of moderate energy to escape. (Thus for 90-Mev incident neutrons Hadley and York[42] find for the production of protons of greater than 20 Mev in C, Cu, and Pb cross sections of 0.41, 0.31, and 0.24 times the respective inelastic cross sections. This decrease they interpret as due to the increased difficulty for a proton to leave the larger nuclei.) For incident neutrons of average energy 300 Mev, Blau, Oliver, and Smith,[43] using stratified emulsions, find that the number of protons of greater than 60 Mev ejected per star in the light and heavy nuclei is approximately the same, indicating the smaller percentage of protons in the larger nuclei which can escape at these energies. At higher energies the effect of cascade action would be expected to predominate, as reflected in the variation of gray-black tracks in our experiment.

For a more detailed treatment, a Goldberger-type analysis of a group of cascades in nuclei of various sizes can be made. Since the mean free path in nuclear matter is, as shown above, in first approximation independent of the nuclear radius, the same diagrams can be used for several elements by redrawing the surface of the nucleus for smaller and smaller nuclei. This has been carried out on a 2-dimensional analysis (of the sort developed by Bernadini *et al.*[37]) for a few interactions by Lindenbaum,[44] but the small number of cases analyzed gives an inconclusive result. The assumptions of the Goldberger model would in any case be very dubious for nuclei as small as $A=14$, since no allowance is made for the alpha-particle structure of the light elements or for the depletion of the nucleus during the cascade, which represents a significant change in the case of small nuclei.

VIII. CONCLUSION

The foil sandwich method described appears to be a valuable tool in studying nuclear disintegrations. Data have been presented on the variation of star size distributions and cross sections with the atomic number of the target nucleus. In addition, the particles of moderate energy attributed to a "knock-on" process were analyzed. The low-energy spectra, excitation energies, "temperatures," and α/p ratios associated with the "evaporation" process, and their variation with atomic number, will be presented and compared with theory upon completion of analysis of low-sensitivity plates which permit more accurate grain counts at low energies and better differentiation between protons and alpha particles. At the other extreme of energy, the foil sandwich method appears to be of limited value in studying very high-energy processes such as meson production, because the detection efficiency for shower particles is low. (Minimum ionization tracks which pass steeply through the emulsion are difficult to detect, whereas those at glancing angles strike the emulsion far from the star center.) A series of foil experiments at cyclotron energies is to be undertaken; use of monoenergetic incident particles permits a more adequate comparison with the theory of the Z dependence of evaporation and knock-on processes than is possible with the variety of particles and energies present in the cosmic radiation. Bombardment with a neutron beam will also permit a much higher star density to be recorded because of the relative absence of the spurious unrelated tracks which determine the maximum exposure allowable in the cosmic-ray sandwich experiments.

The assistance of Mr. Lawrence Greene and Mr. Richard Wilson in analyzing the plates is gratefully acknowledged. The following students also participated in the project: H. Martinek, D. Orr, M. Meux, J. Bailey, M. Jones, and M. Reed.

[40] See, e.g., Fernbach, Serber, and Taylor, Phys. Rev. **75**, 1352 (1949).
[41] J. DeJuren and N. Knable, Phys. Rev. **77**, 606 (1950).
[42] J. Hadley and H. York, Phys. Rev. **80**, 345 (1950).
[43] We are indebted to Dr. Blau for a prepublication copy of this forthcoming paper.
[44] S. Lindenbaum (private communication).